A Journal of the Gesellschaft Deutscher Chemiker

Angewandte International Edition Chemie

GDCh

www.angewandte.org

Accepted Article

Title: Cell Surface Engineering by Phase-Separated Coacervates for Antibody Display and Targeted Cancer Cell Therapy

Authors: Hongfei Chen, Yishu Bao, Xiaojing Li, Fangke Chen, Ryohichi Sugimura, Xiangze Zeng, and Jiang Xia

To be cited as: *Angew. Chem. Int. Ed.* **2024**, e202410566

Link to VoR: https://doi.org/10.1002/anie.202410566

WILEY VCH

10.1002/anie.202410566

WILEY-VCH

RESEARCH ARTICLE

Cell Surface Engineering by Phase-Separated Coacervates for Antibody Display and Targeted Cancer Cell Therapy

Hongfei Chen, [a]† Yishu Bao,[a]† Xiaojing Li,[a] Fangke Chen,[b] Ryohichi Sugimura,[c] Xiangze Zeng,[b] Jiang Xia*, [a]

[a] H. C., Y. B., X. L., J. X.
Department of Chemistry and Center for Cell & Developmental Biology
The Chinese University of Hong Kong
Shatin, Hong Kong SAR, China
E-mail: jiangxia@cuhk.edu.hk
[c] F. C., X. Z.
Department of Physics, Hong Kong Baptist University, Kowloon Tong, Hong Kong SAR, China.
[b] R. S.
School of Biomedical Sciences, The University of Hong Kong, Hong Kong, Hong Kong SAR, China.

† H. C. and Y. B. contribute equally to this work.

Supporting information for this article is given via a link at the end of the document.

Abstract: Cell therapies such as CAR-T have demonstrated significant clinical successes, driving the investigation of immune cell surface engineering using natural and synthetic materials to enhance their therapeutic performance. However, many of these materials do not fully replicate the dynamic nature of the extracellular matrix (ECM). This study presents a cell surface engineering strategy that utilizes phase-separated peptide coacervates to decorate the surface of immune cells. We meticulously designed a tripeptide, Fmoc-Lys-Gly-Dopa-OH (KGdelta; Fmoc = fluorenylmethyloxycarbonyl; delta = Dopa, dihydroxyphenylalanine), that forms coacervates in aqueous solution via phase separation. These coacervates, mirroring the phase separation properties of ECM proteins, coat the natural killer (NK) cell surface with the assistance of Fe^{3+} ions and create an outer layer capable of encapsulating monoclonal antibodies (mAb), such as Trastuzumab. The antibody-embedded coacervate layer equips the NK cells with the ability to recognize cancer cells and eliminate them through enhanced antibody-dependent cellular cytotoxicity (ADCC). This work thus presents a unique strategy of cell surface functionalization and demonstrates its use in displaying cancer-targeting mAb for cancer therapies, highlighting its potential application in the field of cancer therapy.

Introduction

Cell therapies are emerging as a new therapeutic method in biomedicine, generating effective treatments for previously incurable diseases, such as cancers. [1-3] Oftentimes, cells need to be engineered before they can be used in therapies. For example, immune effector cells are engineered by installing molecular guides such as antibodies on the surface to specifically recognize cancer cells for the precise killing of tumors; such an effect has been called antibody-dependent cellular cytotoxicity (ADCC). [4–10] Therapeutic monoclonal antibodies (mAbs) are natural engagers, as immune cells possess Fc-binding receptors to display antibodies on the surface. However, the engaging capability of native mAbs is often very weak. Synthetic engagers, i.e., antibody-derived designer molecules, including bispecific antibodies, biTE, etc., based on chemical or genetic modification of mAbs or antibody-like molecules (such scFv, nanobody, and Fab), have been devised to modify immune effector cells. [11–13] Alternatively, researchers can chemically engineer the surface of immune effector cells and directly embed, display, or conjugate the engagers on the surface of immune effector cells. [14,15] On the other hand, genetic modification of T cells resulted in CAR-T therapies, in which patient-derived T cells were transfected with plasmids expressing chimeric antigen receptors (CARs). As the success of CAR-T has been mostly limited to blood cancers, natural killer (NK) cell-based immunotherapies are gaining growing attention as researchers seek alternatives to T cells. The therapeutic potential of NK cells has been significantly bolstered by enhancing their recognition and cytotoxic capacities. [11, 12, 16-19]

The clinical success of cell therapies has invigorated the exploration of new approaches for cell surface engineering. Chemical strategies for cell surface engineering include decorating the cell surface with natural and synthetic materials, such as nanoparticles, microparticles, and polymeric coatings, to enhance the therapeutic effects of the carrier cells. [20-24] Surface modification arms cells with functionalities unattainable in their naive states, including protection against the hostile environment and clearance rate, enhanced cell trafficking, masking of the cell-surface antigens, modulation of the inflammatory phenotype, and others. [20-24] Regarding the cell types, red blood cells (RBCs) are the most common cells in cell surface engineering. For example, Ferguson and coworkers conjugated two affinity ligands to nanocarriers, one binding RBCs and the other binding targeted pulmonary endothelial cells; the binding of the dual affinity nanocarriers to RBCs leads to lung-targeted enrichment. [25] Glassman and coworkers utilized single-chain-antibody-mediated coupling of liposomes to RBCs to prolong the circulation of the liposomes. [26] Zhao and coworkers developed a strategy of sheltering the epitopes on Rhesus D(RhD)-positive RBCs using a surface-anchored framework. The

10.1002/anie.202410566

RhD-epitope stealth strategy realized the positive-to-negative blood transition of the RhD antigen and brought hope to patients of the rare blood group. [27] We recently functionalized the surface of RBCs with antibody-lipid conjugates for selective drug delivery. [28] Besides RBCs, platelets, fibroblasts, endothelial cells, islet cells, neural stem cells, yeast cells, myoblasts, lymphoblasts, HeLa cells, and even microbes have been surface-engineered. [20] Immune cells such as T cells were also engineered: Tang and coworkers designed cell surface-conjugated protein nanogels as a carrier for an interleukin-15 super-agonist complex and selectively expanded T cells in tumors. [29] Yet, to our knowledge, surface engineering of other immune cells, such as natural killer (NK) cells, is still scarce.

On another note, liquid-liquid phase separation (LLPS) is a physical phenomenon in which molecules forming a liquid solution spontaneously aggregate to form highly concentrated condensates. These condensates appear as microdroplets with well-defined boundaries, exhibiting a rapid concentration change of several orders of magnitudes. Yet the molecules within the concentrated phase dynamically exchange with those in the surrounding diluted phase. Initially recognized as a common occurrence in polymer solutions, LLPS has recently been found in cells, compartmentalizing cellular space and regulating various cellular processes, including gene transcription, the formation of heterochromatin, assembly of the spindle apparatus, asymmetric cell division, autophagy, innate immune response, and many others. [30-37] Most of these phase-separating systems require the participation of biopolymers, such as proteins, nucleic acids, or their combinations, as their interchain interactions fortify the network of the coacervates. [38-43] Many extracellular matrix proteins are known to form liquid-liquid phase separation, including elastin, galectin-3, matrilin-3, *etc*. [44-46] Conceivably, decorating cell surface with molecular coacervates would mimic the extracellular matrix of the cellular microenvironment. Besides biopolymers, recent discoveries found that oligopeptides can also form condensates through phase separation governed by various interactions such as charge-charge, dipole-dipole, cation-π interactions, hydrogen bonds, π-π stacking, biomolecular recognition, and ligand-bridging. [47]

LLPS is also found in the biogenesis of different biomaterials, including various silks, squid beaks, and marine adhesives. [48-50] Mussel foot proteins (Mfps), which were secreted by marine mussels, are rich in a post-translationally modified amino acid L−3,4-dihydroxyphenylalanine (Dopa), which plays an essential role in the phase separation of these proteins (Figure 1A). The adhesive and cohesive properties of Mfps were based on various interactions, including hydrogen bonds, π-π interactions, π-cation interactions, and metal coordination. For example, Mfp-5 is considered the first secreted protein to initiate the wet adhesion of mussels in the process of plaque formation, featuring a very high Dopa content (~30%). In 2023, Yu and coworkers reported a Dopa-containing peptide 16-mer that can form coacervates in seawater. [51] Notably, Guo and coworkers harnessed polyphenols as building blocks to construct superstructures on the surface of cells, which inspired us to design Dopa-containing peptides for cell surface engineering. [52-55]

Here, we report a tripeptide Fmoc-Lys-Gly-Dopa-OH (KGdelta) that forms phase-separated coacervates in the aqueous solution. We study the ability of the peptide coacervates to sequester cargo molecules such as proteins, nucleic acids, and small molecules (Figure 1B). Furthermore, the tripeptide coacervate provides a new way of functionalizing the immune cell surface with antibodies for targeted cancer therapy.

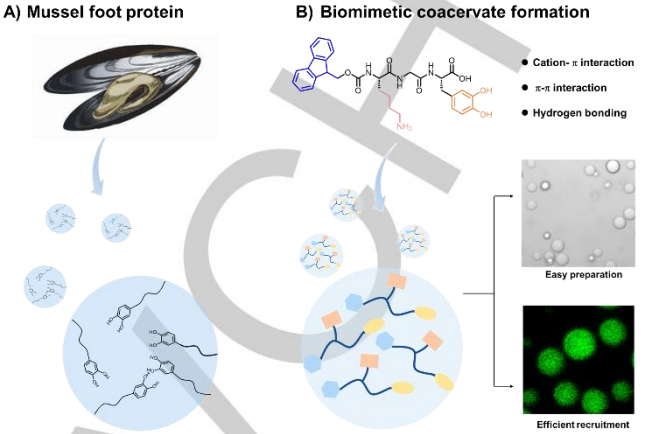

Figure 1. Phase-separating tripeptide inspired by adhesive mussel foot protein. A) Mussel foot proteins exhibit outstanding properties through the Dopa groups, including phase separation. B) Mimicking the phase-separating Mfps, we design Dopa-containing tripeptides that are capable of forming coacervates under biological conditions.

Results and Discussion

1. Screening of a peptide library

A library of tripeptides was designed following the "sticker-and-spacer" model and synthesized. The peptides contain a hydrophobic N-terminal group Fmoc, and a C-terminal aromatic amino acid, either Phe, Tyr, or Dopa. In the middle, a Lys residue contributes its amine side chain to form cation-π interaction, and a Gly residue serves as a flexible spacer between the interacting moieties (Figure 2A). The C-terminal carboxylic acid increases the solubility and supports ionic interaction. When these peptides were dissolved in PBS at pH 7.4, only one tripeptide, Fmoc-Lys-Gly-Dopa-OH (KGdelta), formed microdroplets in the solution. Changing the Dopa group to Tyr or Phe turned the peptides into a solution or gel-like precipitates (Figure S1). Changing the Lys residue to Arg generated gel-like precipitates. Fmoc-His-Gly-Dopa-OH formed microdroplets only in acidic solutions, and Fmoc-Gly-Gly-Dopa-OH gave a clear solution in PBS (Figure S2). Reducing the hydrophobicity of Fmoc increased the solubility of the peptides but also diminished the microdroplet formation. These data indicated a meticulous design for a fine balance between strength and flexibility is critical to forming microdroplets (Table 1).

2. Tripeptide KGdelta forms phase-separated coacervates

We next prove that the KGdelta microdroplets show features of phase-separated coacervation. Microdroplets were formed by diluting the peptide stock solution (100 mg/mL in DMSO or DI H_2O) to 5 mg/mL in PBS (pH 7.4). The solution immediately turned turbid, and microdroplets with sizes up to several microns could be visualized under a microscope (Figure 2B). A control peptide, Fmoc-Lys-Gly-Tyr-OH, dissolved in PBS under the same condition showed as a clear solution (Figure S1). Dynamic light

10.1002/anie.202410566

scattering (DLS) analysis showed microdroplet sizes of several microns. Zeta potential measurement showed that KGdelta coacervates carried positive charges (Figure S3). The microdroplets could be stained with 0.1% (v/v) Sybr Green I. They were highly mobile in the solution and spontaneously coalesced (Figures 2C and S4). We then performed a fluorescence recovery after photobleaching (FRAP) assay. After photobleaching, the fluorescence of the microdroplets recovered to 90% of the signal before bleaching within 100 seconds (Figure 2D). Higher peptide concentration, near neutral pH value (pH 5.5 – 8.5), and salt concentration promoted microdroplet formation (Figure S5). The microdroplet formation was pH switchable: microdroplets were formed at neutral pH but disappeared at an acidic pH reversibly, based on turbidity measurement (Figure 2E). Increasing the temperature from 25℃ to 50℃ led to complete disappearance of the microdroplets (Figure 2F). Taken together, these data show that the KGdelta microdroplets are phase-separated coacervates.

Table 1 I Physical states of synthetic tripeptides

Sequence	Structure	Condensate appearance
Fmoc-Lys-Gly-Dopa-OH	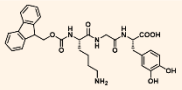	Microdroplets
Fmoc-Lys-Gly-Tyr-OH	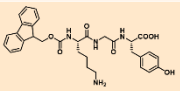	Solution
Fmoc-Lys-Gly-Phe-OH	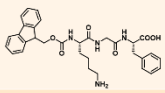	Gel-like precipitates
Fmoc-Gly-Gly-Dopa-OH	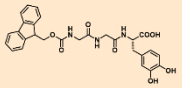	Solution
Fmoc-His-Gly-Dopa-OH	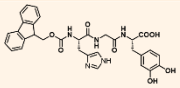	Microdroplets (lower pH ~5.5) Gel-like precipitates (high pH ~9.0)
Fmoc-Arg-Gly-Dopa-OH	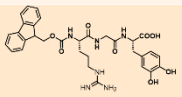	Gel-like precipitates (pH ~3.0, fluorescent)
Fmoc-Lys-Dopa-OH	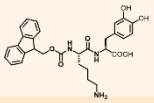	Gel-like precipitates
Ac-Lys-Gly-Dopa-OH	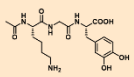	Solution
DPAA-Lys-Gly-Dopa-OH	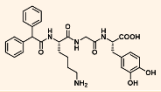	Solution
DPPA-Lys-Gly-Dopa-OH	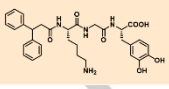	Solution

Table 1. Screening the physical states of a tripeptide library.

We conducted all-atom molecular dynamics simulations to investigate the driving forces leading to the phase separation of the KGdelta peptide. We simulated 10 KGdelta molecules in a water box approximately $7 \times 7 \times 7\ nm^3$ in size. Four independent simulations were performed, each with different starting structures and with a duration of 500 ns. Subsequently, we calculate the distribution of the number density of key functional groups of KGdelta molecules as a function of distance. The number density at a specific distance reflects the likelihood of two molecules remaining at that distance. As shown in Figure 3, distributions of number density for Aro(Fmoc)-Aro(Fmoc), NH_3^+-COO^-, and COO^--OH(Dopa) show higher peaks at short distances than others, indicating more frequent contacts among these groups. These findings suggest that the $\pi-\pi$ interactions between aromatic rings of Fmoc, the electrostatic interactions between Lys and the negatively charged carboxylate group at the C-terminus, and the hydrogen bonding between the carboxylate group and the hydroxyl group of Dopa play key roles in the phase separation of these molecules. These results are consistent with experimental findings that mutations in these key functional groups suppress the phase separation of KGdelta molecules.

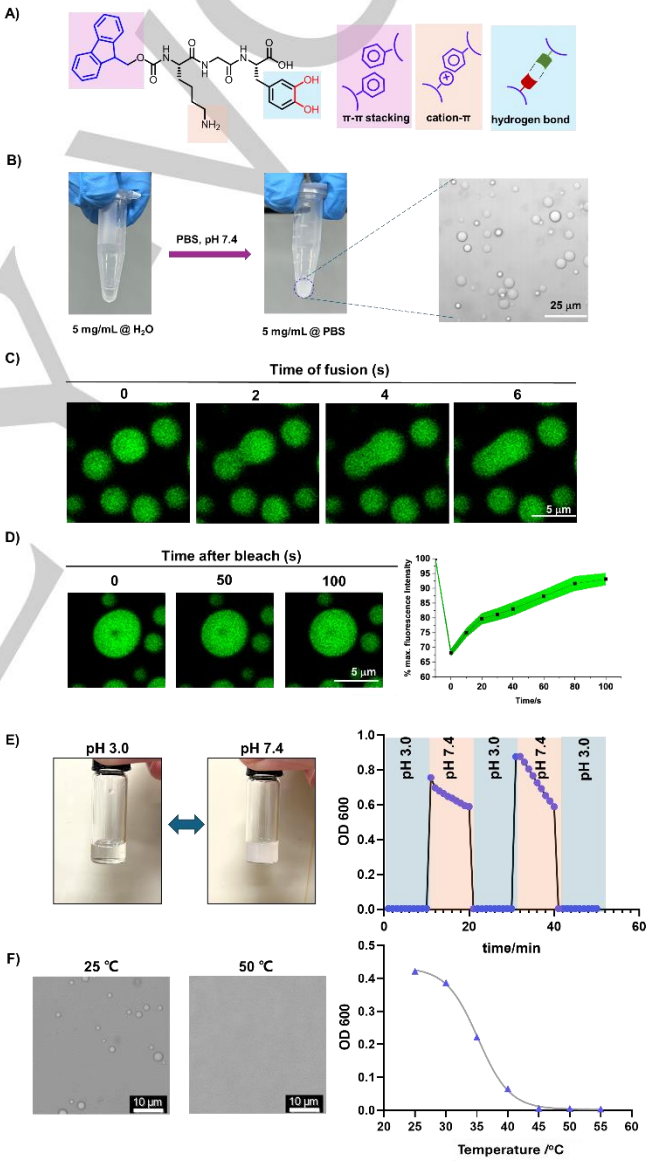

Figure 2. Phase separation properties of the KGdelta coacervates. **A)** Structure of the KGdelta peptide and a schematic illustration of the possible interactions. **B)** Photos and optical microscopic images of the microdroplets formed by KGdelta (5.0 mg/mL in PBS solution). **C)** Fluorescent microscopic images showing the fusion of microdroplets. The droplets were stained by Sybr Green I. **D)** FRAP analysis showing the recovery of the

10.1002/anie.202410566

fluorescence of the microdroplets after photobleaching. Data are presented as the mean ± s.d. of 3 independent experiments, with the s.d. shown in green. **E)** pH-responsiveness of the microdroplet formation, as monitored by turbidity. **F)** Temperature-responsiveness of the microdroplets monitored by turbidity.

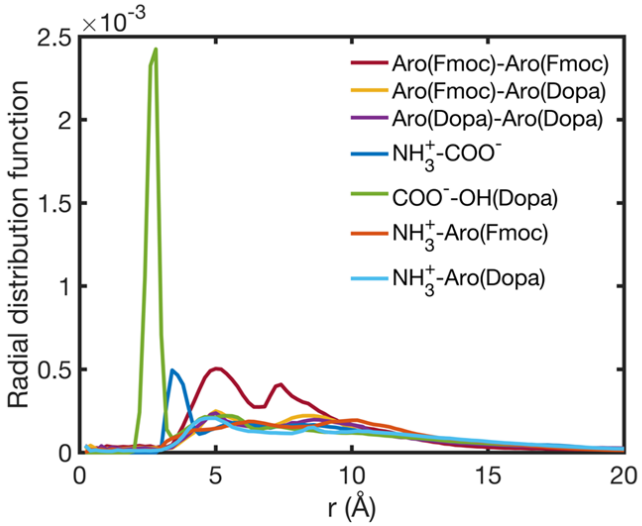

Figure 3. Distribution of number density $n(r)$ of functional groups in KGdelta as a function of distance calculated from all-atom molecular dynamics simulations. Aro(Fmoc) and Aro(Dopa) denote the aromatic rings in Fmoc and Dopa. NH_3^+, COO^-, and OH(Dopa) denote the positively charged ammonium group in Lys, negatively charged carboxylate group in the C-terminus of Dopa, and hydroxyl group in Dopa. Please refer to the supporting information for details of the calculation of $n(r)$.

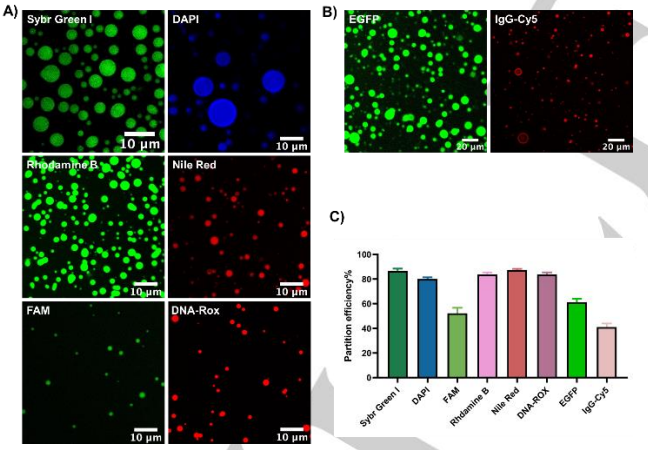

Figure 4. Partitioning and enrichment of guest molecules in KGdelta coacervates. **A)** Confocal fluorescence images of KGdelta coacervates incubated with different fluorescent molecules. **B)** Confocal fluorescence images of KGdelta coacervates incubated with EGFP or IgG-Cy5. **C)** Partition efficiency of different guest molecules in KGdelta coacervates. Briefly, in a solution of protein or small molecule cargo (0.1 mg/mL), the KGdelta peptide was added to a final concentration of 3 mg/mL to form coacervates. The mixture was then centrifuged, and the fluorescent signal of the supernatant was measured as F1. The fluorescent signal of the cargo solution without peptide was measured as F0. The partition efficiency was calculated as (F0-F1)/F0×100%. Data are presented as the mean ± s.d. of 3 independent experiments.

3. Guest recruitment in KGdelta coacervates

Molecular coacervates are known to recruit and enrich guest molecules. [56] We first determined the ability of the KGdelta coacervates to concentrate fluorescent molecules, Sybr Green I, DAPI, rhodamine B (RhoB), Nile red, and fluorescein (FAM) by fluorescence microscopy (Figures 4A and S6). After adding the fluorescent dyes, confocal microscopy images of the coacervates demonstrated strong fluorescence within the microdroplets, indicating their capability to enrich molecular dyes (Figure S7). Apart from small molecule fluorophores, KGdelta coacervates also enriched larger proteins, such as EGFP and antibodies (Figures 4B and S8). Interestingly, for some large coacervates, the IgG-Cy5 seems to enrich on the surface of the microdroplets. The partition efficiencies of these guest molecules in coacervates were calculated (Figure 4C). Despite the zwitterionic and hydrophobic nature of the KGdelta peptide, cationic dyes seem to have higher partition efficiency than the anionic dye FAM and proteins in the coacervates. The cargo also affects the size of the coacervates. The mechanisms, however, are yet unknown. These data show that the KGdelta coacervates can enrich a wide range of molecules, potentially serving as a reservoir for delivery.

4. Cell surface engineering based on KGdelta coacervates and Fe^{3+} ions

Previous studies reported that Fe^{3+} ions could induce metal–phenolic coordination-mediated assembly of the complexes on the cellular surfaces. [57, 58] Therefore, we coated the surface of immune cells with KGdelta coacervates in the presence of Fe^{3+} ion. KGdelta coacervates showed a smaller size in the presence of $FeCl_3$ (Figure S9). The KGdelta coacervates were prepared at a peptide concentration, and the guest protein was partitioned into the coacervates during the preparation. After 3 minutes of incubation between the coacervates and cells, Fe^{3+} ions were added for 10 minutes before washing the cells (Figure 5A). We coated THP1 cells with mCherry-encapsulated KGdelta coacervates and observed a fluorescent layer around THP1 cells (Figure 5B). Control groups without $FeCl_3$ or KGdelta coacervates could not modify the cell surface (Figure S10). The surface coating was successfully implemented in different cells, including macrophages, NK cells, T cells, fibroblast cells, and cancer cells. Fluorescent layers were observed on the surfaces of all these cells, indicating the successful engineering of the cell surface and the presentation of the fluorescent proteins on the cell surface assisted by the peptide coacervates (Figure 5C). Besides, different proteins, such as BSA, streptavidin, and IgG, were coated on the cell surface using the same protocol (Figure 5D). These results show that Dopa-containing KGdelta coacervates, with the assistance of Fe^{3+}, provide a viable material to engineer the surface of mammalian cells. This coating strategy seems non-toxic to the cells (Figure S11).

5. Enhanced ADCC via cell surface functionalization

Lastly, the coacervate-based cell-surface engineering strategy was applied to display Trastuzumab, an FDA-approved anti-HER2 monoclonal antibody, on the immune cell surface for enhanced antibody-dependent cellular cytotoxicity (ADCC) (Figure 6A). [9, 10] THP1 cells were coated with Trastuzumab for 20 min in the presence of the KGdelta coacervates and Fe^{3+}. After extensive washing to remove unreacted reagents, THP1 cells coated with Trastuzumab-embedded coacervates and labeled

10.1002/anie.202410566

with the green dye DIO (THP1-Tras) were mixed and incubated with HER2-positive SKOV3 cells (labeled with the red dye Mito Tracker Red) for 8 hours. THP1 cells without coating with Trastuzumab were used as a control. Because SKOV3 cells are adherent and THP1 cells form suspension culture, no THP1 cells could be found on the coverslip in the control group after the washing step. In contrast, THP1-Tras cells attached to SKOV3 cells after the washing step, showing that Trastuzumab displayed on the surface of THP1-Tras cells guided THP1 to SKOV3 and formed contacts between the two cells (Figure 6B). 3D confocal microscopic images showed enhanced cell-cell interaction between THP1-Tras and SKOV3 cells (Figure 6C). Next, we utilized the same protocol to functionalize NK-92 cells, a type of interleukin-2 (IL-2)-dependent NK cell line with cellular cytotoxicity but without targeting capability. Based on the release of lactate dehydrogenase (LDH), at an effector cells/target cells (E/T) ratio of 3:1, Trastuzumab-coated NK-92 cells (NK-92-Tras) showed significantly higher cytotoxicity than NK-92 cells without coating with Trastuzumab (Figure 6D). Such an enhanced ADCC effect was found to be HER2-dependent because NK-92-Tras cells did not effectively kill HER2-negative MDA-MB-231 cells. Taken together, our experiments show that the coacervate-based surface functionalization of immune effector cells enables the display of HER2-specific antibody Trastuzumab, promotes the contact between immune effector cells and the target cancer cells, and enhances the killing of the cancer cells.

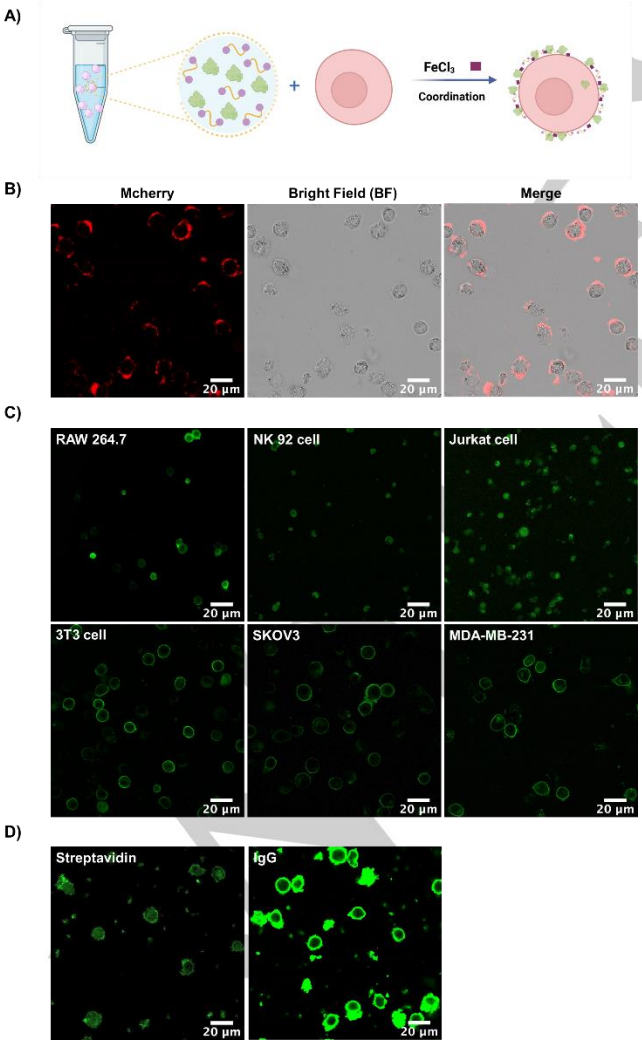

Figure 5. Cell surface engineering by KGdelta coacervates. **A)** Schematic diagram of the cell surface functionalization by KGdelta coacervates assisted by Fe^{3+}. **B)** Confocal microscopic images of the THP1 cells coated with KGdelta coacervates (red represents the mCherry protein). **C)** Surface functionalization of different cell types by fluorescently labeled BSA (with Alexa Fluor 488 through NHS-amine reaction). **D)** Cell surface functionalization with streptavidin and IgG covalently fluorescently labeled by NHS-Alexa Fluor-488.

CONCLUSIONS

In summary, we report a Dopa-containing tripeptide KGdelta that undergoes phase separation and forms coacervates with liquid-like fluidity. The coordination of Dopa and Fe^{3+} drives the assembly of KGdelta coacervates on the surface of cells, displaying the encapsulated cargo on the cell surface. The formation of coacervate "corona" around cells mimics the extracellular matrix of the cellular microenvironment. Here, we showcase one application of the cell surface engineering strategy using the peptide coacervates. An anti-HER2 mAb Trastuzumab embedded within the coacervate corona on immune cells enhanced the binding between immune cells and HER2+ cancer cells. The surface-engineered NK cells recognized HER2+ cancer cells and exhibited enhanced cytotoxicity through the ADCC effect. Taken together, we have shown here a tripeptide that forms molecular coacervates based on phase separation, presented a unique cell-surface engineering strategy, and showcased a potential application in guiding the immune effector cells to recognize and kill HER2+ cancer cells. Notwithstanding, how the antibodies were displayed inside the coacervates and how they mediate the interaction between two cells are yet unknown to us. We speculate that the antibodies will adopt a random orientation when embedded inside the coacervates, and a subpopulation will be at the right orientation to bind to cancer cells. Nevertheless, our work shows that coacervates may be a new type of material for cell surface functionalization to endow immune effector cells with new therapeutic potential.

Experimental Section

Experimental Procedures and Figures S1-S12 and Table S1 are included in the Supporting Information.

Acknowledgments

This work was partially funded by grants from the University Grants Committee of Hong Kong (GRF grants 14304320, 14306222, and 14301922), Research Impact Fund R5013-19, and CUHK (ICSG, CRIMS, and Direct Grant 4053563). XZ acknowledges funding from the University Grants Committee of Hong Kong (ECS 22302823) and the National Natural Science Foundation of China (Young Scientist Fund 22303073).

Keywords: Cell surface engineering • phase separation • coacervate • natural killer cells • cancer therapy

10.1002/anie.202410566

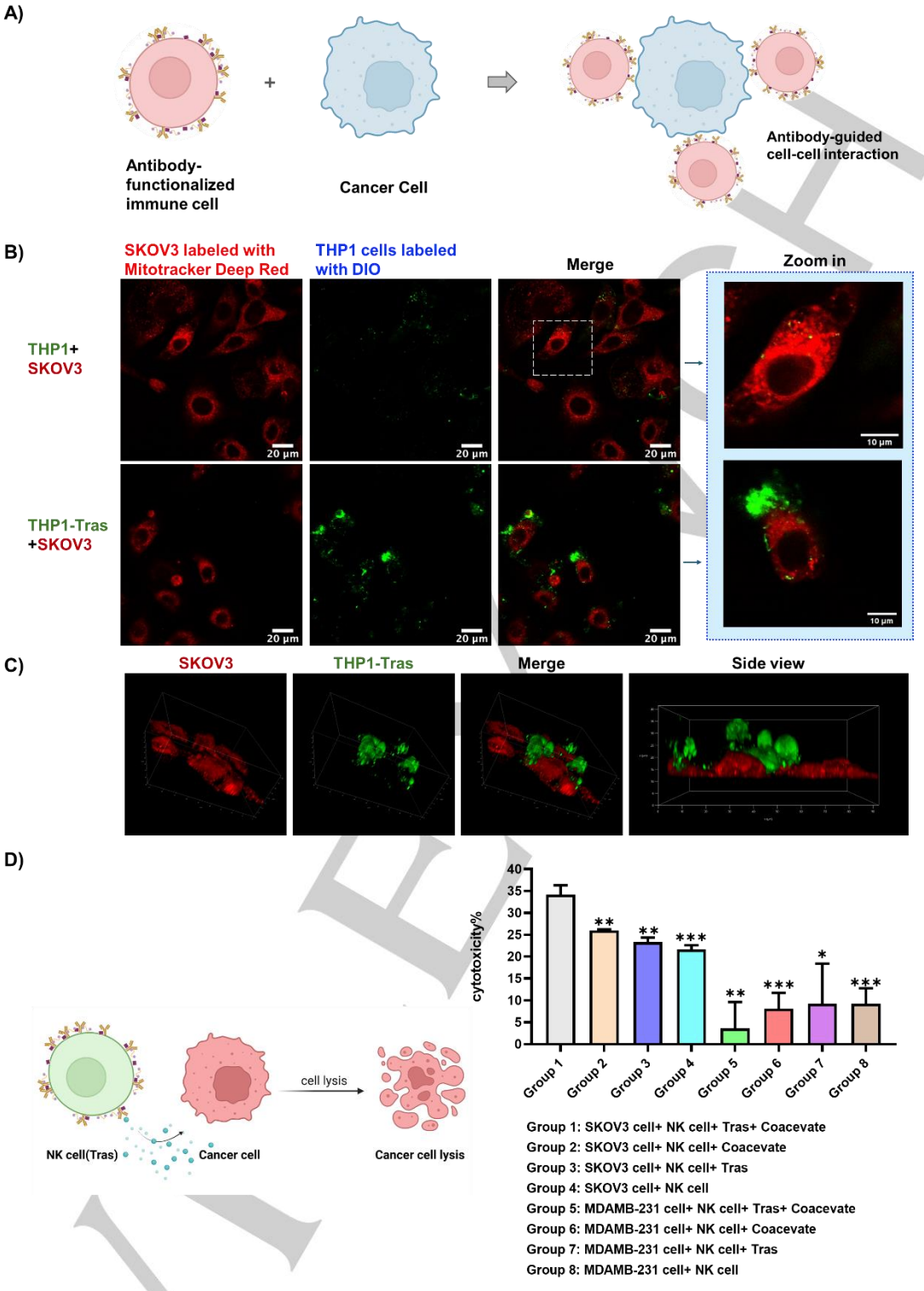

Figure 6. Enhanced ADCC via cell surface functionalization by antibody-embedded KGdelta coacervates. A) Schematic diagram showing the surface-functionalized immune cells bind to cancer cells through surface-displayed antibodies. B) Confocal microscopic images showing the interaction of THP1-Tras with HER2+ SKOV3 cells. C) 3D view images showing the interaction of THP1-Tras with HER2+ SKOV3 cells. D) Cytotoxicity of the cancer cells measured in different co-culture groups. Data are presented as the mean ± s.d. of n = 3 independent experiments. *, P <0.05. **, P <0.01. ***, P < 0.001.****, P <0.0001 relative to Group 1.

References

1. El-Kadiry, A. E.; Rafei, M.; Shammaa R. Cell Therapy: Types, Regulation, and Clinical Benefits. *Front. Med.* **2021**, *8*, 756029.
2. Bashor, C. J.; Hilton, I. B.; Bandukwala, H.; Smith, D. M.; Veiseh O. Engineering the next generation of cell-based therapeutics. *Nat. Rev. Drug Discov*. **2022**, *21*, 655-675.
3. Irvine, D. J.; Maus, M. V.; Mooney, D. J.; Wong, W. W. The future of engineered immune cell therapies. *Science* **2022**, *378*, 853-858.
4. Saeed, A. F.; Wang, R.; Ling, S.; Wang, S. Antibody Engineering for Pursuing a Healthier Future. *Front. Microbiol.* **2017**, *8*, 495.
5. Zinn, S.; Vazquez-Lombardi, R.; Zimmermann, C.; Sapra, P.; Jermutus, L.; Christ, D. Advances in antibody-based therapy in oncology. *Nat. Cancer*. **2023,** *4*, 165-180.
6. Jin, S.; Sun, Y.; Liang, X.; Gu, X.; Ning, J.; Xu, Y.; Chen, S.; Pan, L. Emerging new therapeutic antibody derivatives for cancer treatment. *Sig. Transduct. Target. Ther.* **2022,** *7*, 39.
7. Goydel, R. S.; Rader, C. Antibody-based cancer therapy. *Oncogene* **2021,** *40*, 3655-3664.
8. Scott, A. M.; Wolchok, J. D.; Old, L. J. Antibody therapy of cancer. *Nat. Rev. Cancer.* **2012,** *12*, 278-287.
9. Gómez Román, V. R.; Murray, J. C.; Weiner, L. M. Antibody-Dependent Cellular Cytotoxicity (ADCC). In Antibody Fc: Linking Adaptive and Innate Immunity; Ackerman, M. E., Nimmerjahn, F., Eds.; Academic Press, **2014**; pp 1-27.
10. Igietseme, J. U.; Zhu, X.; Black, C. M. Fc Receptor-Dependent Immunity. In Antibody Fc: Linking Adaptive and Innate Immunity; Ackerman, M. E., Nimmerjahn, F., Eds.; Academic Press, **2014**; pp 269-281.
11. Gauthier, L.; Morel, A.; Anceriz, N.; Rossi, B.; Blanchard-Alvarez, A.; Grondin, G.; Trichard, S.; Cesari, C.; Sapet, M.; Bosco, F.; Rispaud-Blanc, H.; Guillot, F.; Cornen, S.; Roussel, A.; Amigues, B.; Habif, G.; Caraguel, F.; Arrufat, S.; Remark, R.; Romagné, F.; Morel, Y.; Narni-Mancinelli, E.; Vivier, E. Multifunctional Natural Killer Cell Engagers Targeting NKp46 Trigger Protective Tumor Immunity. *Cell* **2019**, *177*, 1701-1713.
12. Xiao, X.; Cheng, Y.; Zheng, X.; Fang, Y.; Zhang, Y.; Sun, R.; Tian, Z.; Sun, H. Bispecific NK-cell engager targeting BCMA elicits stronger antitumor effects and produces less proinflammatory cytokines than T-cell engager. *Front. Immunol.* **2023,** *14*, 1-13.
13. Goebeler, M.-E.; Bargou, R. C. T cell-engaging therapies — BiTEs and beyond. *Nat. Rev. Clin. Oncol.* **2020**, *17*, 418-434.
14. Sterner, R. C.; Sterner, R. M. CAR-T cell therapy: current limitations and potential strategies. *Blood Cancer J.* **2021**, *11*, 69.
15. Milone, M. C.; Xu, J.; Chen, S. J.; Collins, M. A.; Zhou, J.; Powell, D. J., Jr.; Melenhorst, J. J. Engineering enhanced CAR T-cells for improved cancer therapy. *Nat. Cancer.* **2021,** *2*, 780-793.
16. Romero D. Promising early results with CAR NK cells. *Nat. Rev. Clin. Oncol*. **2024**, *21*, 168.
17. Liu, S.; Galat, V.; Galat, Y.; Lee, Y. K. A.; Wainwright, D.; Wu, J. NK cell-based cancer immunotherapy: from basic biology to clinical development. *J. Hematol. Oncol.* **2021**, *14*, 7.
18. Vivier, E.; Rebuffet, L.; Narni-Mancinelli, E.; Cornen, S.; Igarashi, B. Y.; Fantin, V. R. Natural killer cell therapies. *Nature* **2024**, *626*, 727–736.
19. Bashor, C. J.; Hilton, I. B.; Bandukwala, H.; Smith, D. M.; Veiseh, O. Engineering the next generation of cell-based therapeutics. *Nat. Rev. Drug Discov*. **2022**, *21*, 655–675.
20. Adebowale, K.; Liao, R.; Suja, V. C.; Kapate, N.; Lu, A.; Gao, Y.; Mitragotri, S. Materials for cell surface engineering. *Adv. Mater*. **2023**, 2210059.
21. Abbina, S.; Siren, E. M. J.; Moon, H.; Kizhakkedathu, J. N. Surface engineering for cell-based therapies: techniques for manipulating mammalian cell surfaces. *ACS Biomater. Sci. Eng.* **2018**, *4*, 3658-3677.
22. Almeida-Pinto, J.; Lagarto, M. R.; Lavrador, P.; Mano, J. F.; Gaspar, V. M. Cell surface engineering tools for programming living assemblies. *Adv. Sci.* **2023**, *10*, e2304040.
23. Stevens, M. M.; George, J. H. Exploring and engineering the cell surface interface. *Science* **2005**, *310*, 1135-8.
24. Mager, M. D.; LaPointe, V.; Stevens, M. M. Exploring and exploiting chemistry at the cell surface. *Nat. Chem*. **2011**, *3*, 582-9.
25. Ferguson, L. T.; Hood, E. D.; Shuvaeva, T.; Shuvaev, V. V.; Basil, M. C.; Wang, Z.; Nong, J.; Ma, X.; Wu, J.; Myerson, J. W.; Marcos-Contreras, O. A.; Katzen, J.; Carl, J. M.; Morrisey, E. E.; Cantu, E.; Villa, C. H.; Mitragotri, S.; Muzykantov, V. R.; Brenner, J. S. Dual affinity to RBCs and target cells (DART) enhances both organ- and cell type-targeting of intravascular nanocarriers. *ACS Nano* **2022**, *16*, 4666-4683.
26. Glassman, P. M.; Villa, C. H.; Marcos-Contreras, O. A.; Hood, E. D.; Walsh, L. R.; Greineder, C. F.; Myerson, J. W. Targeted in vivo loading of red blood cells markedly prolongs nanocarrier circulation. *Bioconjug. Chem.* **2022**, *33*, 1286-1294.
27. Zhao, Y.; Fan, M.; Chen, Y.; Liu, Z.; Shao, C.; Jin, B.; Wang, X.; Hui, L.; Wang, S.; Liao, Z.; Ling, D.; Tang, R.; Wang, B. Surface-anchored framework for generating RhD-epitope stealth red blood cells. *Sci. Adv*. **2020**, *6*, eaaw9679.
28. Li, B.; Yuan, D.; Chen, H.; Wang, X.; Liang, Y.; Wong, C.T.T.; Xia, J. Site-selective antibody-lipid conjugates for surface functionalization of red blood cells and targeted drug delivery. *J. Controll. Release* **2024**, *370*, 302-309.
29. Tang, L.; Zheng, Y.; Melo, M. B.; Mabardi, L.; Castaño, A. P.; Xie, Y. Q.; Li, N.; Kudchodkar, S. B.; Wong, H. C.; Jeng, E. K.; Maus, M. V.; Irvine, D. J. Enhancing T cell therapy through TCR-signaling-responsive nanoparticle drug delivery. *Nat. Biotechnol*. **2018**, *36*, 707-716.
30. Dobry, A. B.-K., F., Phase separation in polymer solution. *J. Polymer Sci.* **1947**, *2*, 90-100.
31. Hu, W. (2013). Polymer Phase Separation. In: Polymer Physics. Springer, Vienna.
32. Alberti, S.; Hyman, A. Biomolecular condensates at the nexus of cellular stress, protein aggregation disease and ageing. *Nat. Rev. Mol. Cell Biol.* **2021**, *22*, 196-213.
33. Shin, Y.; Brangwynne, C. P. Liquid phase condensation in cell physiology and disease. *Science* **2017**, *357*, eaaf4382.
34. Mehta, S.; Zhang, J. Liquid–liquid phase separation drives cellular function and dysfunction in cancer. *Nat. Rev. Cancer* **2022**, *22*, 239-252.
35. Boeynaems, S.; Alberti, S.; Fawzi, N. L.; Mittag, T.; Polymenidou, M., Rousseau, F.; Schymkowitz, J., Shorter, J.; Wolozin, B., Van Den Bosch L, Tompa P, Fuxreiter M. Protein Phase Separation: A New Phase in Cell Biology. *Trends Cell Biol*. **2018**, *28*, 420-435.
36. Alberti, S.; Dormann, D. Liquid-Liquid Phase Separation in Disease. *Annu. Rev. Genet.* **2019**, *53*, 171-194.
37. Perry, S. L. Phase separation: Bridging polymer physics and biology. *Curr. Opin. Colloid Interface Sci.* **2019**, *39*, 86-97.
38. Gao, Z. Z.; Chang, W.; Zhang, R.; Yang, S.; Zhao, G. Liquid-liquid phase separation: unraveling the enigma of biomolecular condensates in microbial cells. *Front. Microbiol.* **2021**, *12*, 751880.
39. Brangwynne, C. P.; Eckmann, C. R.; Courson, D. S.; Rybarska, A.; Hoege, C.; Gharakhani, J.; Jülicher, F.; Hyman, A. A. Germline P granules are liquid droplets that localize by controlled dissolution/condensation. *Science* **2009**, *324*, 1729-1732.
40. Wang, Y.; Liu, M.; Wei, Q.; Wu, W.; He, Y.; Gao, J.; Zhou, R.; Jiang, L.; Qu, J.; Xia, J. Phase-separated multienzyme compartmentalization for terpene biosynthesis in a prokaryote. *Angew. Chem. Int. Ed.* **2022**, *61*, e202203909.
41. Schuster, B. S.; Regy, R. M.; Dolan, E. M.; Ranganath, A. K.; Jovic, N.; Khare, S. D.; Shi, Z.; Mittal, J. Biomolecular condensates: sequence determinants of phase separation, microstructural organization, enzymatic activity, and material properties. *J. Phys. Chem. B* **2021**, *125*, 3441-3451.
42. Qian, Z.-G.; Huang, S.-C.; Xia, X.-X. Synthetic protein condensates for cellular and metabolic engineering. *Nat. Chem. Biol.* **2022**, *18*, 1330-1340.
43. Li, P.; Banjade, S.; Cheng, H. C.; Kim, S.; Chen, B.; Guo, L.; Llaguno, M.; Hollingsworth, J. V.; King, D. S.; Banani, S. F.; Russo, P. S.; Jiang, Q. X.; Nixon, B. T.; Rosen, M. K. Phase transitions in the assembly of multivalent signalling proteins. *Nature* **2012**, *483*, 336-340.
44. Muiznieks, L. D.; Sharpe, S.; Pomès, R.; Keeley, F. W. Role of Liquid-Liquid Phase Separation in Assembly of Elastin and Other Extracellular Matrix Proteins. *J. Mol. Biol.* **2018**, *430*, 4741-4753.

45. Chiu, Y.-P.; Sun, Y.-C.; Qiu, D.-C.; Lin, Y.-H.; Chen, Y.-Q.; Kuo, J.-C.; Huang, J.-R. Liquid-liquid phase separation and extracellular multivalent interactions in the tale of galectin-3. *Nat. Commun*. **2020**, *11*, 1229.
46. Huang, Y.; Xu, X.; Lu, Y.; Sun, Q.; Zhang, L.; Shao, J.; Chen, D.; Chang, Y.; Sun, X.; Zhuo, W.; Zhou, T. The phase separation of extracellular matrix protein matrilin-3 from cancer-associated fibroblasts contributes to gastric cancer invasion. *FASEB J*. **2024**, *38*, e23406.
47. Abbas, M.; Lipiński, W. P.; Wang, J.; Spruijt, E. Peptide-based coacervates as biomimetic protocells. *Chem. Soc. Rev.* **2021**, *50*, 3690-3705.
48. Malay, A. D.; Suzuki, T.; Katashima, T.; Kono, N.; Arakawa, K.; Numata, K. Spider silk self-assembly via modular liquid-liquid phase separation and nanofibrillation. *Sci. Adv.* **2020**, *6*, eabb6030.
49. Gabryelczyk, B.; Cai, H.; Shi, X.; Sun, Y.; Swinkels, P. J. M.; Salentinig, S.; Pervushin, K.; Miserez, A.; Hydrogen bond guidance and aromatic stacking drive liquid-liquid phase separation of intrinsically disordered histidine-rich peptides. *Nat. Commun*. **2019**, *10*, 5465.
50. Zhao, H.; Sun, C.; Stewart, R. J.; Waite, J. H. Cement proteins of the tube-building polychaete Phragmatopoma californica. *J. Biol. Chem*. **2005**, *280*, 42938–42944.
51. Guo, Q.; Zou, G.; Qian, X.; Chen, S.; Gao, H.; Yu, J., Hydrogen-bonds mediate liquid-liquid phase separation of mussel derived adhesive peptides. *Nat. Commun*. **2022**, *13*, 5771.
52. Guo, J.; Suástegui, M.; Sakimoto, K. K.; Moody, V. M.; Xiao, G.; Nocera, D. G.; Joshi, N. S. Light-driven fine chemical production in yeast biohybrids. *Science* **2018**, *362*, 813-816.
53. Guo, J.; Tardy, B. L.; Christofferson, A. J.; Dai, Y.; Richardson, J. J.; Zhu, W.; Hu, M.; Ju, Y.; Cui, J.; Dagastine, R. R.; Yarovsky, I.; Caruso, F. Modular assembly of superstructures from polyphenol-functionalized building blocks. *Nat. Nanotechnol*. **2016**, *11*, 1105-1111.
54. Pan, J.; Gong, G.; Wang, Q.; Shang, J.; He, Y.; Catania, C.; Birnbaum, D.; Li, Y.; Jia, Z.; Zhang, Y.; Joshi, N. S.; Guo, J. A single-cell nanocoating of probiotics for enhanced amelioration of antibiotic-associated diarrhea. *Nat. Commun.* **2022**, *13*, 2117.
55. Zhang, Y.; Wang, J.; He, Y.; Pan, J.; Jin, X.; Shang, J.; Gong, G.; Richardson, J. J.; Manners, I.; Guo, J. Customizable Supraparticles Constructed from Catechol-Terminated Molecular Building Blocks with Controllable Intermolecular Interactions. *Angew. Chem. Int. Ed.* **2023**, *62*, e202303463.
56. Bao, Y.; Chen, H.; Xu, Z.; Gao, J.; Jiang, L.; Xia, J. Photo-Responsive Phase-Separating Fluorescent Molecules for Intracellular Protein Delivery. *Angew. Chem. Int. Ed.* **2023**, *62*, e202307045.
57. Guo, J.; Tardy, B.; Christofferson, A.; Dai, Y.; Richardson, J. J.; Zhu, W.; Hu, M.; Ju, Y.; Cui, J.; Dagastine, R. R.; Yarovsky, I.; Caruso, F. Modular assembly of superstructures from polyphenol-functionalized building blocks. *Nat. Nanotech*. **2016**, *11*, 1105-1111.
58. Zhang, C.; Wu, B.; Zhou, Y.; Zhou, F.; Liu, W.; Wang, Z. Mussel-inspired hydrogels: from design principles to promising applications. *Chem. Soc. Rev.* **2020**, *49*, 3605-3637.

10.1002/anie.202410566

WILEY-VCH

RESEARCH ARTICLE

Entry for the Table of Contents

Insert graphic for Table of Contents here.

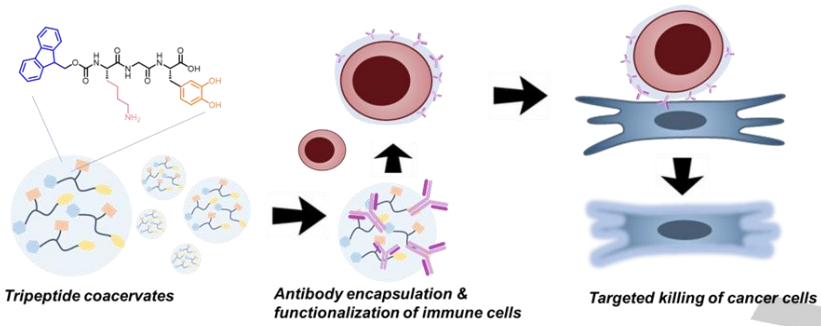

Insert text for Table of Contents here.

Tripeptide forms phase-separated coacervates, which functionalize the surface of NK cells, display an anti-HER2 mAb within the coacervate layer on the cell surface, and guide the NK cells to recognize and kill HER2+ cancer cells.